

Supplementary Information

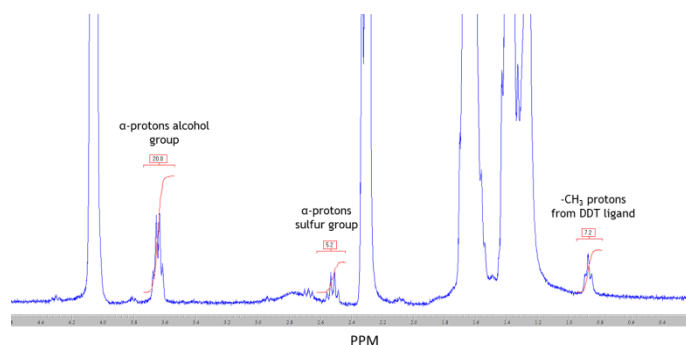


Fig. S1. $^1\text{H-NMR}$ from 4.5-0.2 PPM of $\text{CuInS}_2/\text{ZnS}$ QDs after ligand exchange with oligo-CL ligands.

Integrated in the $^1\text{H-NMR}$ spectrum the $-\text{CH}_3$ end-group of remaining DDT ligands at 0.9-0.8PPM (3 protons) and the α -protons of the $-\text{OH}$ end group of the oligo-CL ligands at 3.7-3.6PPM (2 protons). Based on the integrals of the peaks the conversion of the ligand exchange can be estimated accordingly:

$$\text{Conversion (\%)} = \frac{\frac{\int_{3.7\text{PPM}}}{\# \text{ protons}}}{\frac{\int_{3.7\text{PPM}}}{\# \text{ protons}} + \frac{\int_{0.9\text{PPM}}}{\# \text{ protons}}} * 100\%$$

$$\text{Conversion (\%)} = \frac{\frac{\int_{2.0}}{2}}{\frac{\int_{2.0}}{2} + \frac{\int_{7.2}}{3}} * 100\%$$

Conversion (%) = ~ 80%.

In the $^1\text{H-NMR}$ spectrum a broad peak at 2.9-2.6PPM was observed that was later on assigned to ligands bound to the QD surface (Fig. 5). The quartet at 2.5PPM was assigned to the thiol end group α -protons of ligands in solution. From the ratio of the alcohol α -protons to the thiol α -protons it followed that about 25% of the ligand was free in solution. A small triplet was observed at 2.7PPM on the position of the α -protons of the disulfide, suggesting a few percent of oxidized ligands.

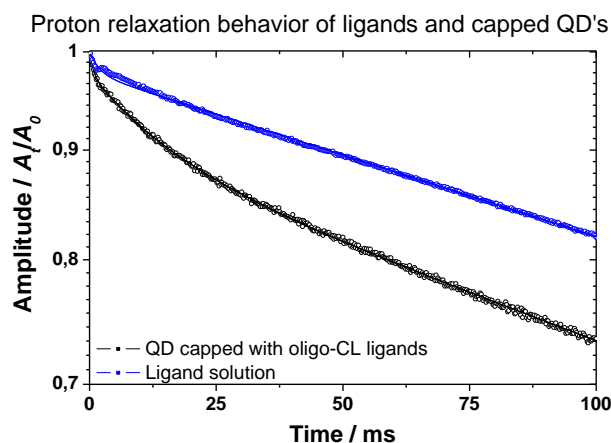


Fig. S2. Solid state NMR T_2 relaxometry of oligo-CL ligands in d-chloroform compared to $\text{CuInS}_2/\text{ZnS}$ QDs after ligand exchange with oligo-CL ligands.

Solid-state NMR relaxometry was applied to investigate the relaxation behavior of the oligo-CL ligand free in CDCl_3 solution as well as of QDs with the oligo-CL ligands. The longitudinal relaxation behavior of the oligo-CL ligands free in solution fitted well to an exponential function with a T_1 relaxation time constant of 635 ± 5 ms, a typical value for solutions of low molecular weight oligomeric compounds. While in contrast the recovery curve of the QDs with the oligo-CL ligands deviated from the expected exponential behavior, and therefore only an average T_1 relaxation time constant of 590 ± 10 ms could be determined accurately. The decrease in T_1 could be due to slightly lower molecular mobility of bound ligands to the QDs and/or due to the presence of paramagnetic ions which leached from the QDs and acted as relaxation agents. To further investigate the molecular mobility, T_2 relaxation experiments were performed (Fig. S2), the oligo-CL ligand in solution had a T_2 relaxation time constant of 570 ± 1 ms comparable to the T_1 as expected for ligands in solution with a fast rotational and translational mobility. QDs with oligo-CL ligands showed a complex T_2 relaxation decay which deviated from the exponential decay. The decay was fitted with exponential functions with three components representing the following relaxation times: 0.7 ± 0.1 ms (2.2 ± 0.2 %); 15.9 ± 0.4 ms (7.8 ± 0.1 %) and 487 ± 2 ms (90 ± 0.2 %). The multi-component relaxation behavior was attributed to heterogeneous mobility of ligands reversely bound to the QDs surface. However no rigid or semi-rigid material was observed using a solid-echo experiment, which could possibly be explained by heterogeneous magnetic behavior close to the surface of the QDs.

Transmission of polymer film and QD composite

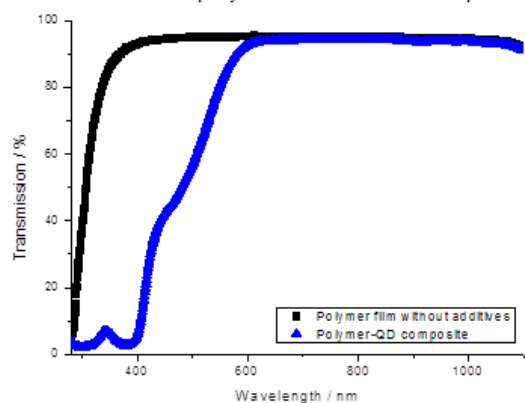


Fig. S3. Transmission spectrum of a cured QD composite and a reference film without QDs. The transmission of the film with embedded QDs showed a reduced transmittance below 600nm which was attributed to light absorption by the QDs. The transmission >600nm was comparable to the blank polymer film without QDs. This observation indicated that the QDs and small QD aggregates in the film did not cause additional reflections.

Fluorescence lifetime

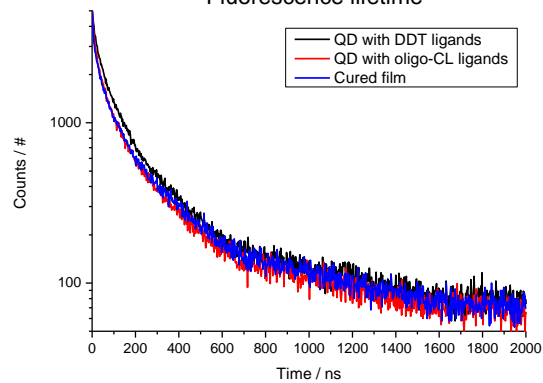


Fig. S4. Fluorescence lifetime of QDs with DDT and oligo-CL ligands and of a composite films.

S5 Theoretical model description

The applied theoretical model was based on the model as described by Rothermund et al.^{25,26} For a detailed description please consult the original articles. Briefly the model divides the incoming solar radiation into a transmitted and an absorbed and down-shifted photon fraction. By a multiplication with the cells EQE at respectively the original and down-shifted wavelength for the transmitted and down-shifted light fraction the current generation can be calculated after LDS.

The theoretical model specifies a down-shifting efficiency term (η_{LDS}) which comprises additional factors for loss due to reflection (R), the QY (η_{QY}), out-coupling loss (η_{out}) and loss due to re-absorption (η_{abs}) according to Equation S1.

$$\eta_{LDS} = (1 - R) \cdot \eta_{QY} \cdot (1 - \eta_{out}) \cdot (1 - \eta_{abs}) \quad (1)$$

Whereas η_{out} was calculating according Snell's law in steradians (Equation S2) with n_{air} and n_{medium} the refractive indices of respectively air and the LDS layer.

$$\eta_{out} = \frac{(1 - \cos(\sin^{-1}(\frac{n_{air}}{n_{medium}}))) \cdot 2\pi}{4\pi} \quad (2)$$

The fraction of re-absorbed light was calculated from the spectral overlap of the absorption and emission spectrum according Equation S3. With $Em(\lambda)$ the relative emission intensity per wavelength and $T(\lambda)$ the transmission at that wavelength.

$$\eta_{abs} = \frac{\int (Em(\lambda) \cdot (1 - T(\lambda)) d\lambda)}{\int Em(\lambda) d\lambda} \quad (3)$$

The I_{SC} of a PV cell can be approximated by multiplying the EQE of the cell with the photon flux of the solar spectrum and the elemental electron charge (q) and integrating over the full range where the cell has a response. The theoretical I_{SC} after incorporation of a LDS layer can be calculated in a similar way according Equation S4 with P_{abs} the absorbed photon fraction in the LDS layer, $EQE(\lambda_{em})$ the EQE at the emission wavelength of the LDS additive, P_{trans} the transmitted photon fraction.

$$I_{SC} = q \int P_{abs} \cdot \eta_{LDS} \cdot EQE(\lambda_{em}) + P_{trans} \cdot EQE(\lambda) d\lambda \quad (4)$$